http://journal.uir.ac.id/index.php/JGEET

E-ISSN : 2541-5794
P-ISSN : 2503-216X

Journal of Geoscience,
Engineering, Environment, and Technology
Vol 11 No 1 2026

RESEARCH ARTICLE

Improvement of Earthquake Source Mechanism Using Waveform Inversion in the Indo-Australian Oceanic Plate

Nurma Aisyah[1,*], Muksin[2], Nazli[2], Wahyu Sandriadi[3]

[1] *Master of Physics Departement, Faculty of Mathematics and sciences, Universitas Syiah Kuala, Banda Aceh, Indonesia.*
[2] *Departement of Physics, faculty of Mathematics and Sciences, Universitas Syiah Kuala, Banda Aceh, Indonesia.*
[3] *Departement of Geophysical Engineering, Faculty of Engineering, Universitas Syiah Kuala, Banda Aceh, Indonesia.*

* Corresponding author : nurmaaisyah17@gmail.com
Tel.: +62 851-3581-9419
Received: Jul 28, 2025; Accepted: Mar 13, 2026.
DOI: 10.25299/jgeet.2026.11.1.24276

Abstract

The Indo-Australian Oceanic Plate region is an active and complex subduction zone. Tectonic activity in this area generates various types of faults, including thrust, strike-slip, and normal faults, reflecting the dynamic deformation of the lithosphere. This study aims to refine earthquake source parameters using waveform inversion based on the Bayesian Bootstrap approach. Seven earthquake events with magnitudes greater than 5, occurring between 2010 and 2025, were analyzed to obtain more accurate parameters, including location, depth, origin time, duration, magnitude, and fault plane orientation (strike, dip, and slip). Waveform data were retrieved from the USGS catalog and processed using the Grond and Pyrocko software. The inversion results indicate significant shifts in initial parameters, with misfit values below 0.5, demonstrating a high level of agreement between synthetic and observed waveforms. The tectonic interpretation of the inversion outcomes reveals a relationship between hypocenter depth, fault type, and subduction zone geometry. This research is expected to contribute to a better understanding of earthquake source mechanisms and serve as a scientific reference for disaster mitigation efforts in the Indo-Australian Plate region.

Keywords: Indo-Australian Plate, waveform inversion, Grond, earthquake parameters, focal mechanism.

1. Introduction

Subduction is the process of interaction between two tectonic plates, in which one plate descends beneath the other. The plate that subducts is referred to as the slab, forming a subduction zone that is highly susceptible to earthquakes, posing significant challenges in geoscience studies (Stern, 2002). The subduction between the Indo-Australian Plate and the Sundaland Plate extends from the Andaman Sea, across the Sunda Trench, to Nusa Tenggara and the Java Trench (McCaffrey, 2009).

The subduction rate in this subduction zone ranges from 44 to 48 mm per year (De Mets et al., 2010). This rate can change following the occurrence of an earthquake (Wang et al., 2012). This plate convergence zone is located along the Sumatra-Java-Bali-Lombok Trench (Gibbons et al., 2015; Van Hinsbergen et al., 2018), where the Australian Plate subducts beneath the island arc along the continental margin, moving eastward and rotating counterclockwise in the Banda Sea (Müller et al., 2019). Large earthquakes from the subduction zone can also affect more distant regions as a result of the ongoing plate interactions within the subduction system (Petersen et al., 2004). The movement of these major plates influences the Indonesian archipelago, making the region highly prone to seismic hazards. Such tectonic activity also generates faults, local fractures, and folds, further increasing its vulnerability to natural disasters. The earthquake source mechanism is one of the key aspects in understanding the impacts of subduction processes. Analysis of the earthquake source mechanism, such as fault type, slip direction, and fault plane orientation, is crucial for characterizing and assessing the potential hazards associated with earthquakes (Hall, 2002).

Surface displacement is a key parameter for understanding tectonic deformation along subduction zones, and GNSS provides precise, continuous measurements of crustal motion enabling the quantification of plate convergence, interseismic strain, and deformation related to megathrust locking (Alif, 2024). Research by Alif et al., (2021) further shows that the 2016 M7.8 Indian Ocean earthquake altered plate velocities and increased compressional strain at several GNSS stations, highlighting how large earthquakes can modify plate motion dynamics and indicate the presence of microtectonic blocks such as the Sumatra Block. These results indicate dynamic changes in tectonic plate motion, which are relevant for further analysis of earthquake source mechanisms, particularly through waveform inversion approaches (Lubis et al., 2020).

The earthquake source mechanism is the fault-plane solution represented in a coordinate system. The focal mechanism describes fault orientation and slip, serving as key parameters for determining fault geometry and stress regime. Computational analysis of source mechanisms is commonly interpreted through focal sphere diagrams, or "beach balls," where the pattern indicates the fault type responsible for the earthquake (Shearer, 2009). Such modeling provides parameters including magnitude, origin time, depth, energy release, and fault-plane characteristics. Emphasizes that focal mechanisms are an essential tool for interpreting subsurface geological structures and the stress conditions that control earthquake occurrence (Frohlich, 2001). The earthquake mechanism is controlled by the

propagation pattern of seismic waves within the earth (Sunarjo, 2012).

Seismic waves are energy that propagates through the Earth as a result of an earthquake. They consist of body waves (P and S) that travel through the Earth's interior and surface waves (Rayleigh and Love) that propagate along the upper layers, and are important for earthquake analysis and seismic hazard assessment (Reynolds, 2011; Hidayati 2010). Synthetic waveform modeling is further utilized for automatic inversion to determine the earthquake moment tensor using the Grond software, yielding the strike, dip, and slip of the fault plane as inputs for focal mechanism determination and fault-plane orientation visualization (Cesca et al., 2017). The full-waveform inversion method for determining the seismic moment tensor is capable of providing a far more detailed spatial reconstruction of earthquake sources compared to conventional approaches (Amad et al., 2020).

This study employs the moment tensor inversion method with a Bayesian Bootstrap approach. This approach not only produces the best-fit solution but also provides a distribution of solutions that reflects the uncertainty and variability of the model parameters (Heimann et al., 2018). Furthermore, waveform-based moment tensor inversion plays a crucial role in improving the accuracy of earthquake parameter estimations, including origin time, location, magnitude, event duration, and focal depth. Information derived from moment tensor inversion is also valuable for identifying fault geometry through strike, dip, and slip parameters (Petersen et al., 2021; DeMets et al., 2010). Considering the seismic history of the Indo-Australian Plate, focal mechanism studies are essential for disaster mitigation assessments.

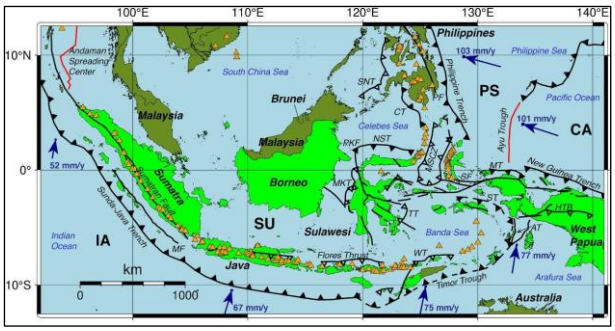

Fig 1. Tectonic Plate Map of the Indo-Australian Plate (Harris, 2021)

These instructions are to be followed strictly, and it is strongly advised to use the styles indicated in this document between square brackets. It is strongly advised NOT to use formatting or styles in your paper different from the ones mentioned here.

2. Methodology

This study utilizes seismicity data and observational waveform data from waveform inversion analysis. The seismicity data are obtained from the USGS earthquake catalog. The catalog provides information such as event time, date, coordinates (latitude and longitude), magnitude, RMS, azimuthal gap, location, and recording seismic stations. To retrieve the USGS catalog, several parameters were specified, including origin time, magnitude, coordinates, depth, and regional boundaries. The seismicity dataset used in this study covers earthquakes occurring between 2010 and 2025 in the vicinity of the Indo-Australian Plate.

The observational waveform data used for inversion and analysis were also obtained from the USGS catalog in miniSEED format with magnitudes greater than 5. These data were downloaded using open-source Python scripts with the Pyrocko library, where parameters such as coordinates, origin time limits, and minimum magnitude thresholds were defined. The outputs include miniSEED waveform files, source parameter information, and station metadata, which allow evaluation of the station–epicenter distance range for each recorded event.

The purpose of using cross-correlation is to obtain optimal time or phase alignment, which strengthens the relationship between the observed and synthetic seismograms. The results of this process are expected to produce a more accurate model that reflects the physical conditions at the earthquake source (Qadariyah et al., 2018). This study employs moment tensor inversion with a Bayesian Bootstrap approach to investigate earthquake source mechanisms in the Indo-Australian Plate. The Bayesian full moment tensor inversion approach is capable of providing more reliable estimates of earthquake source mechanisms, particularly for induced seismicity events (Gu et al., 2018). Seismicity data from the USGS earthquake catalog (2010–2025) and waveform data with magnitudes >5 were collected in miniSEED format using the Pyrocko library. Preprocessing involved preparing waveform files, Green's functions, and earthquake parameters, with signal filters adjusted according to event magnitude. Pyrocko, for the utilization of pre-computed Green's functions, enables seismic wave modeling and source inversion in a fast, accurate, and efficient manner (Heimann et al., 2019). Inversion was performed using the Grond software with 50,000 iterations, where the best-fit solution was determined from the Probability Density Function (PDF). Solutions with misfit values below 0.5 were considered reliable (Petersen, 2021). The final outputs included refined earthquake parameters—magnitude, depth, strike, dip, and slip—along with waveform fitting, moment tensor decomposition, and focal mechanism solutions illustrated as beach-ball diagrams. Understanding the activity in the subduction zone is crucial for risk mitigation and disaster preparedness planning (Irwandi et al., 2025).

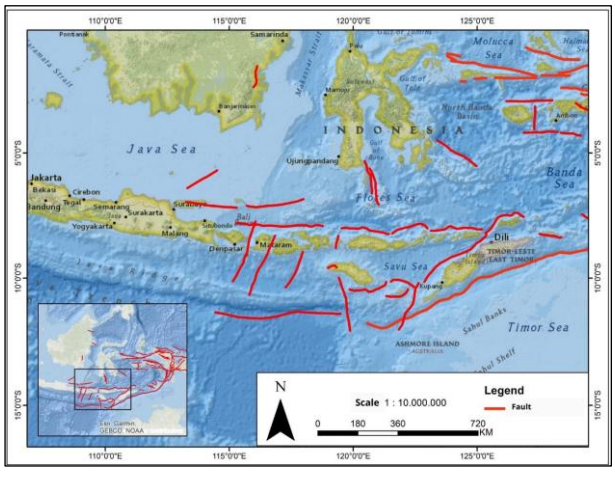

Fig 2. Research Location Map

3. Result and Discussion

The analysis of earthquake parameter refinement is divided into six sections represented by six cross-section profiles from the seven earthquake events. Each cross-section represents the distribution and pattern of the

earthquake parameters from the analyzed events. The data used in this study consist of seismicity records from 2010 to 2025, focusing on seven earthquake events with magnitudes greater than 5. The selection of seismicity data with magnitudes above 5 was specifically conducted to examine the fault characteristics associated with the distribution of large earthquakes around the Indo-Australian Plate. The collected waveform data were prepared for inversion analysis using a Bayesian bootstrap approach. Data analysis was carried out through full-waveform analysis with waveform inversion, resulting in refined earthquake source parameters. The refinement process involved fitting between observed and synthetic waveforms; when the two showed close agreement, the resulting data were considered reliable. The cross-section profiles and the overall distribution of the earthquakes are presented in Figure 3.

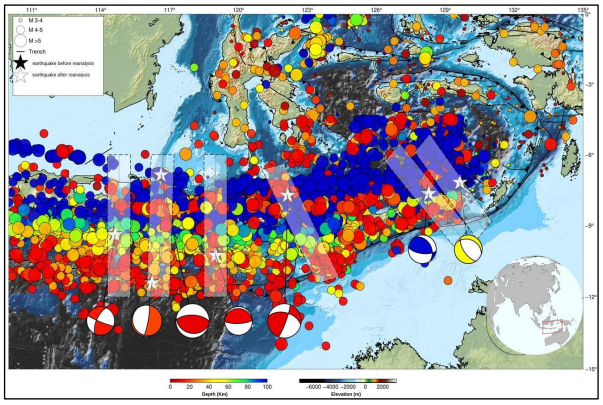

Fig 3. Earthquake Seismicity Distribution in the Surrounding Region of the Indo-Australian Plate

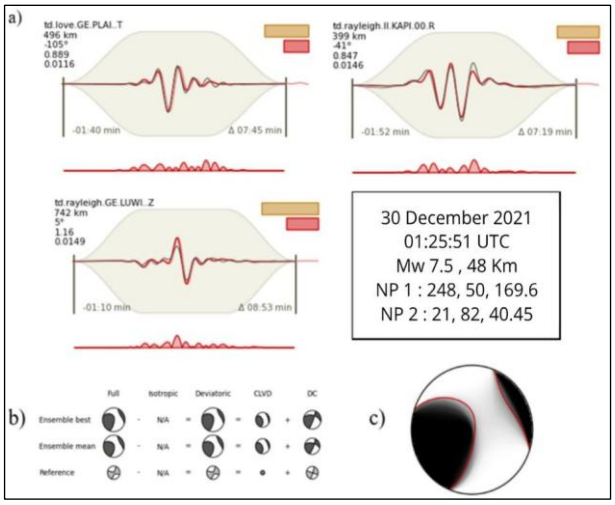

Fig 4. (a) Waveform fitting results (b) MT Decomposition (c) Fuzzy MT of the 2021 Flores earthquake

Figure 3 shows the distribution of earthquake depths in the Indo-Australian Plate region. The colors of the earthquake symbols represent hypocentral depths, where red indicates shallow earthquakes (less than 20 km), while blue represents deeper events (up to >80 km). This variation in earthquake depth is caused by differences in geological and tectonic processes occurring in each area. Shallow earthquakes are generally associated with local fault activity in the upper crust, whereas deeper earthquakes are closely related to the subduction of the oceanic plate beneath the continental or micro-plates, which transports lithospheric material into the mantle. These differences reflect the complex plate dynamics in the Indo-Australian Plate region. The six cross-section profiles represent the seven analyzed earthquakes, with each section marked by a transparent plane perpendicular to the subduction zone direction and interpreted using focal mechanisms.

Figure 4 presents the results of the waveform inversion for the Flores earthquake on December 30, 2021. Synthetic waveforms (red) closely match the observed waveforms (black), indicating reliable inversion results. Station GE.PLAI (T component) shows the best fit with a misfit of 0.01 and ~90% accuracy, while station II.KAPI (R component) has a misfit of 0.014 (~87% accuracy) with minor phase shifts. Station GE.LUWI (Z component) reaches 97% accuracy with a misfit of 0.01, confirming highly reliable data. Figures 4b and 4c show the focal mechanisms derived from Nodal Plane I (248, 50, 169.6) and Nodal Plane II (21, 82, 40.45). Waveform inversion quality can also be evaluated using the Probability Density Function (PDF) for various earthquake parameters, as shown in Figure 5.

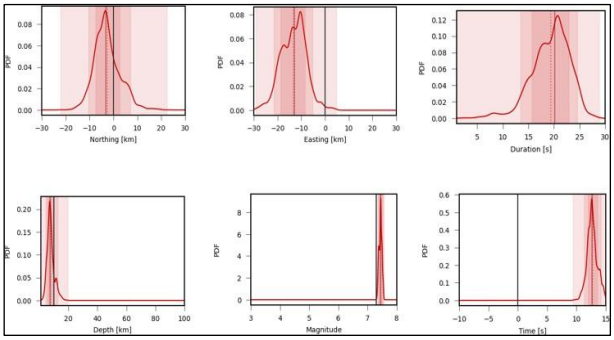

Fig 5. Probability Density Function (PDF) in histogram form for the 2021 Flores earthquake.

The PDF results indicate high-quality waveform inversion, with a tightly clustered median distribution. Figure 5 shows a high PDF, confirming that the parameter corrections are reliable. The inversion results reveal that the 2021 Flores earthquake epicenter shifted 5.8 km south and 10.1 km west from the initially recorded location. The earthquake duration increased by 0.8 s, and the depth changed from 10 km to 48 km, indicating a deeper source than previously estimated. The estimated magnitude reached 7.45 Mw, classifying it as a major earthquake, and the origin time was delayed by 11.5 seconds compared to the initial estimate.

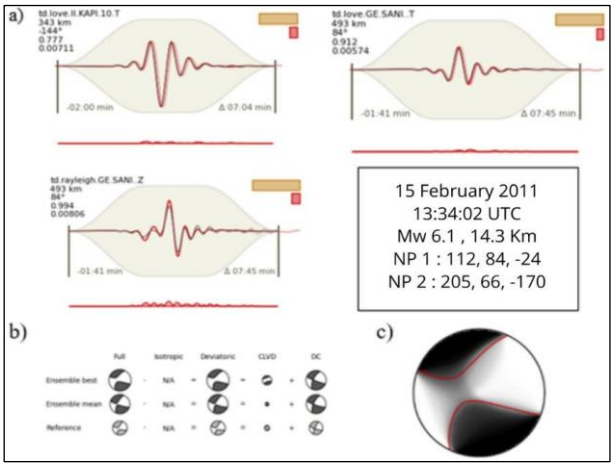

Fig 6. (a) Waveform fitting results (b) MT Decomposition (c) Fuzzy MT of the 2011 Waingapu earthquake

The 2011 Waingapu earthquake parameters were refined using a 0.006–0.025 Hz bandpass filter and 50,000 iterations of waveform inversion, resulting in a final misfit of 0.4 Hz. Station II.KAPI (T component) showed the best fit (misfit 0.007, ~97% accuracy), followed by GE.SANI (T, misfit 0.005, ~98% accuracy) and GE.SANI (Z, misfit 0.008), confirming reliable inversion results. Figures 6b and 6c present the focal mechanisms derived from Nodal Plane I (112, 84, -24) and Nodal Plane II (205, 66, -170).

The inversion results indicate that the 2011 Waingapu earthquake epicenter shifted 5.1 km south and 4.9 km east from its initial location, with the duration increasing by 8.7s. The depth changed from 33 km to 14.3 km, indicating a shallower source than previously estimated. The estimated magnitude reached 6.1 Mw, classifying it as a major earthquake, and the origin time was delayed by 2 s compared to the initial estimate.

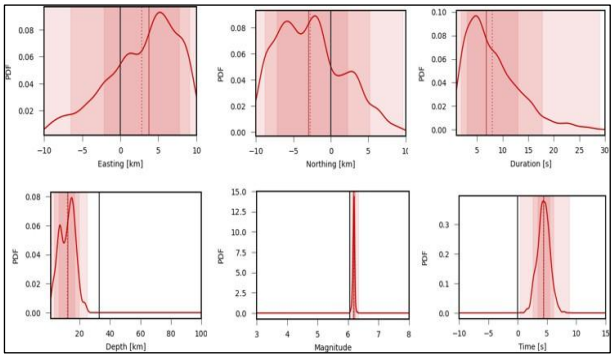

Fig 7. Probability Density Function (PDF) in histogram form for the 2011 Waingapu earthquake

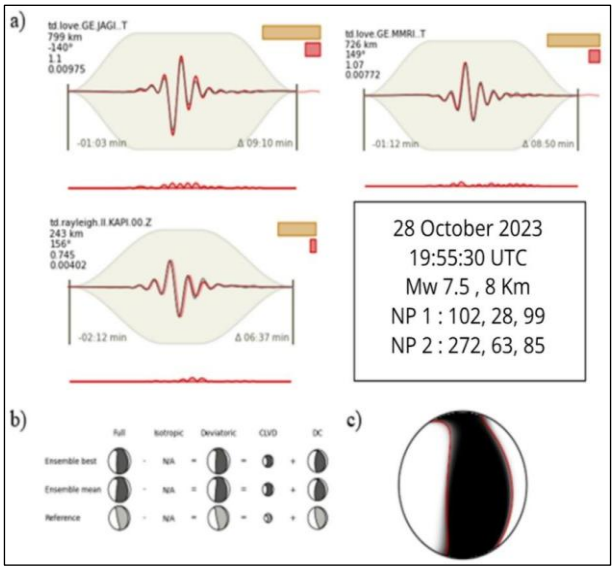

Fig 8. (a) Waveform fitting results (b) MT Decomposition (c) Fuzzy MT of the 2023 Bali earthquake

The waveform inversion for the Bali Sea earthquake on October 28, 2023, shows high reliability. Station GE.JAGI (T component) achieved the best fit (misfit 0.009), followed by GE.MMRI (T, misfit 0.007, ~95% accuracy) and II.KAPI (Z, misfit 0.004), confirming good agreement between synthetic and observed waveforms. Figures 8b and 8c display the focal mechanisms derived from Nodal Plane I (102, 28, 99) and Nodal Plane II (272, 63, 85).

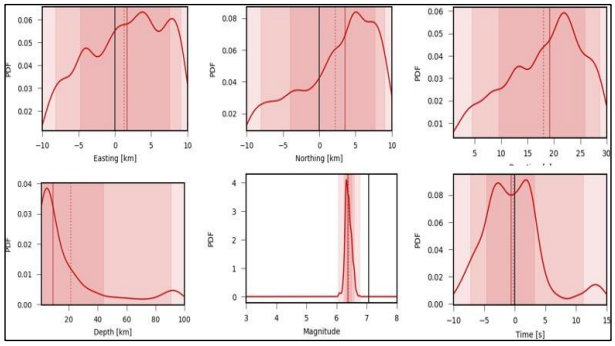

Fig 9. Probability Density Function (PDF) in histogram form for the 2023 Bali earthquake

The inversion results indicate that the 2023 Bali Sea earthquake epicenter shifted 7.8 km north and 4.4 km east from its initial location, with a duration of 20.6 s. The depth changed from 10 km to 8 km, indicating a shallower source than previously estimated. The estimated magnitude reached 7.1 Mw, classifying it as a major earthquake, and the origin time differed by 3 s compared to the initial estimate.

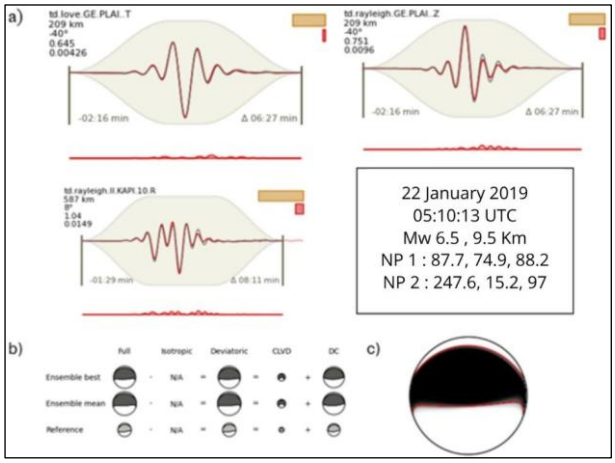

Fig 10. (a) Waveform fitting results (b) MT Decomposition (c) Fuzzy MT of the 2019 Sumba earthquake

In Figure 10a, the best-fitting quality is observed at station GE.PLAI (T component) with a misfit of 0.004, where nearly the entire synthetic waveform follows the observed waveform with ~98% accuracy. GE.PLAI (Z component) also shows good fitting with a misfit of 0.009, while station II.KAPI (R component) exhibits reasonable agreement with a misfit of 0.01. Figures 10b and 10c present the focal mechanisms of the Sumba earthquake on January 22, 2019, derived from Nodal Plane I (87.7, 74.9, 88.2) and Nodal Plane II (247.6, 15.2, 97).

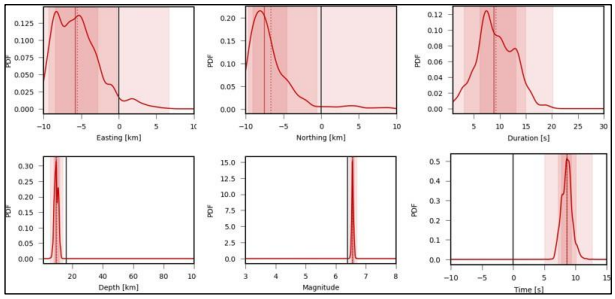

Fig 11. Probability Density Function (PDF) in histogram form for the 2019 Sumba earthquake

The inversion results indicate that the 2019 Sumba earthquake epicenter shifted 7.9 km south and 8.3 km west from its initial location, with a duration of 7.7 s. The depth changed from 16 km to 9.5 km, indicating a shallower source than previously estimated. The estimated magnitude reached 6.53 Mw, classifying it as a major earthquake, and the origin time differed by 3 s compared to the initial estimate.

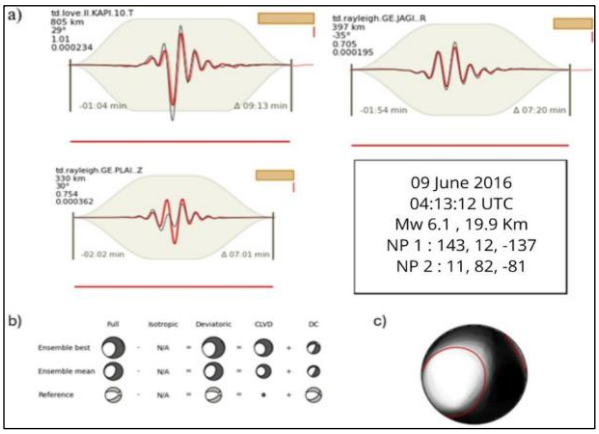

Fig 12. (a) Waveform fitting results (b) MT Decomposition (c) Fuzzy MT of the 2016 Sumbawa earthquake

In Figure 12a, the best-fitting quality is observed at station II.KAPI (T component) with a misfit of 0.002, showing reasonably good agreement despite some waveform discrepancies. Station GE.JAGI (R component) also exhibits good fitting with a misfit of 0.0001 and ~90% accuracy, while GE.PLAI (Z component) shows reasonable agreement with a misfit of 0.0003. Figures 12b and 12c present the focal mechanisms of the Sumbawa earthquake on June 9, 2016, derived from Nodal Plane I (143, 12, -137) and Nodal Plane II (11, 82, -81).

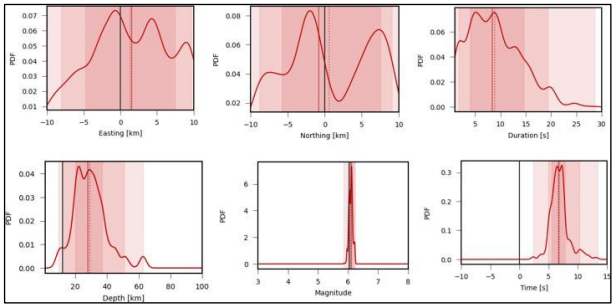

Fig 13. Probability Density Function (PDF) in histogram form for the 2016 Sumbawa earthquake

In Figure 13, the inversion results indicate that the 2016 Sumbawa earthquake epicenter shifted 2.1 km south and 1.9 km east from its initial location, with a duration of 5.6 s. The depth changed from 12 km to 19.9 km, indicating a deeper source than previously estimated. The estimated magnitude reached 6.1 Mw, classifying it as a major earthquake, and the origin time differed by 2 s compared to the initial estimate.

In Figure 14a, the best-fitting quality is observed at station GE.JAGI (T component) with a misfit of 0.009, showing reasonably good agreement despite some waveform discrepancies. Station GE.LUWI (Z component) also exhibits good fitting with a misfit of 0.01 and ~90% accuracy, while II.KAPI (Z component) shows reasonable agreement with a misfit of 0.004. Figures 14b and 14c present the focal mechanisms of the Tanimbar earthquake on August 12, 2013, derived from Nodal Plane I (146, 63, -72) and Nodal Plane II (291, 32, -120).

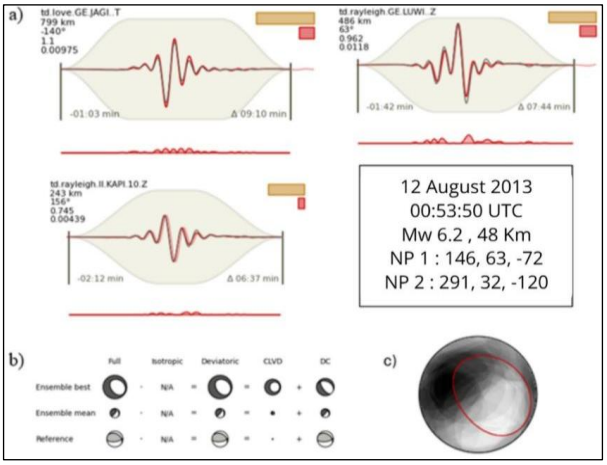

Fig 14. (a) Waveform fitting results (b) MT Decomposition (c) Fuzzy MT of the 2013 Tanimbar earthquake

The inversion results indicate that the 2013 Tanimbar earthquake epicenter shifted 5 km north and 19 km west from its initial location, with a duration of 23.2 s. The depth changed from 109 km to 48 km, indicating a shallower source than previously estimated. The estimated magnitude reached 6.2 Mw, classifying it as a major earthquake, and the origin time differed by 6 s compared to the initial estimate.

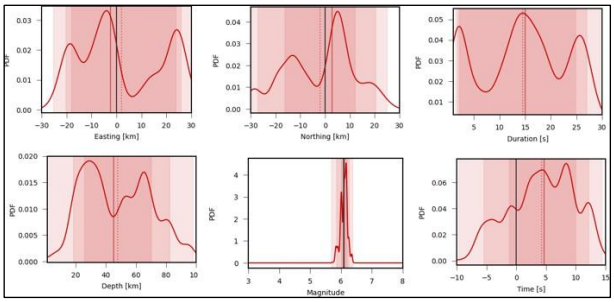

Fig 15. Probability Density Function (PDF) in histogram form for the 2013 Tanimbar earthquake

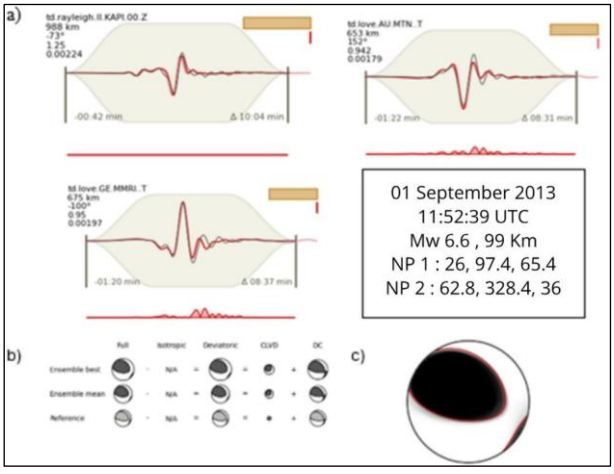

Fig 16. (a) Waveform fitting results (b) MT Decomposition (c) Fuzzy MT of the 2013 Lospales earthquake

In Figure 16a, the best-fitting quality is observed at station II.KAPI (Z component) with a misfit of 0.002, showing reasonably good agreement despite some waveform discrepancies. Station AU.MTN (T component)

and GE.MMRI (T component) also exhibit good fitting with misfits of 0.001, confirming reasonable agreement between synthetic and observed waveforms. Figures 16b and 16c present the focal mechanisms of the Lospales earthquake on September 1, 2013, derived from Nodal Plane I (26, 97.4, 65.4) and Nodal Plane II (62.8, 328.4, 36).

The waveform inversion results for the Lospales earthquake indicate a well-constrained PDF, confirming that the parameter corrections are reliable and acceptable (Figure 17). The inversion shows that the 2013 Lospales earthquake epicenter shifted 8.2 km south and 4.8 km east from its initial location, with a duration of 26 s. The depth changed from 127 km to 99 km, indicating a shallower source than previously estimated. The estimated magnitude reached 6.6 Mw, classifying it as a major earthquake, and the origin time differed by 2 s compared to the initial estimate.

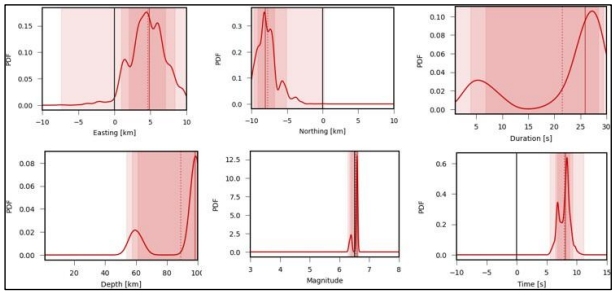

Fig 17. Probability Density Function (PDF) in histogram form for the 2013 Tanimbar earthquake

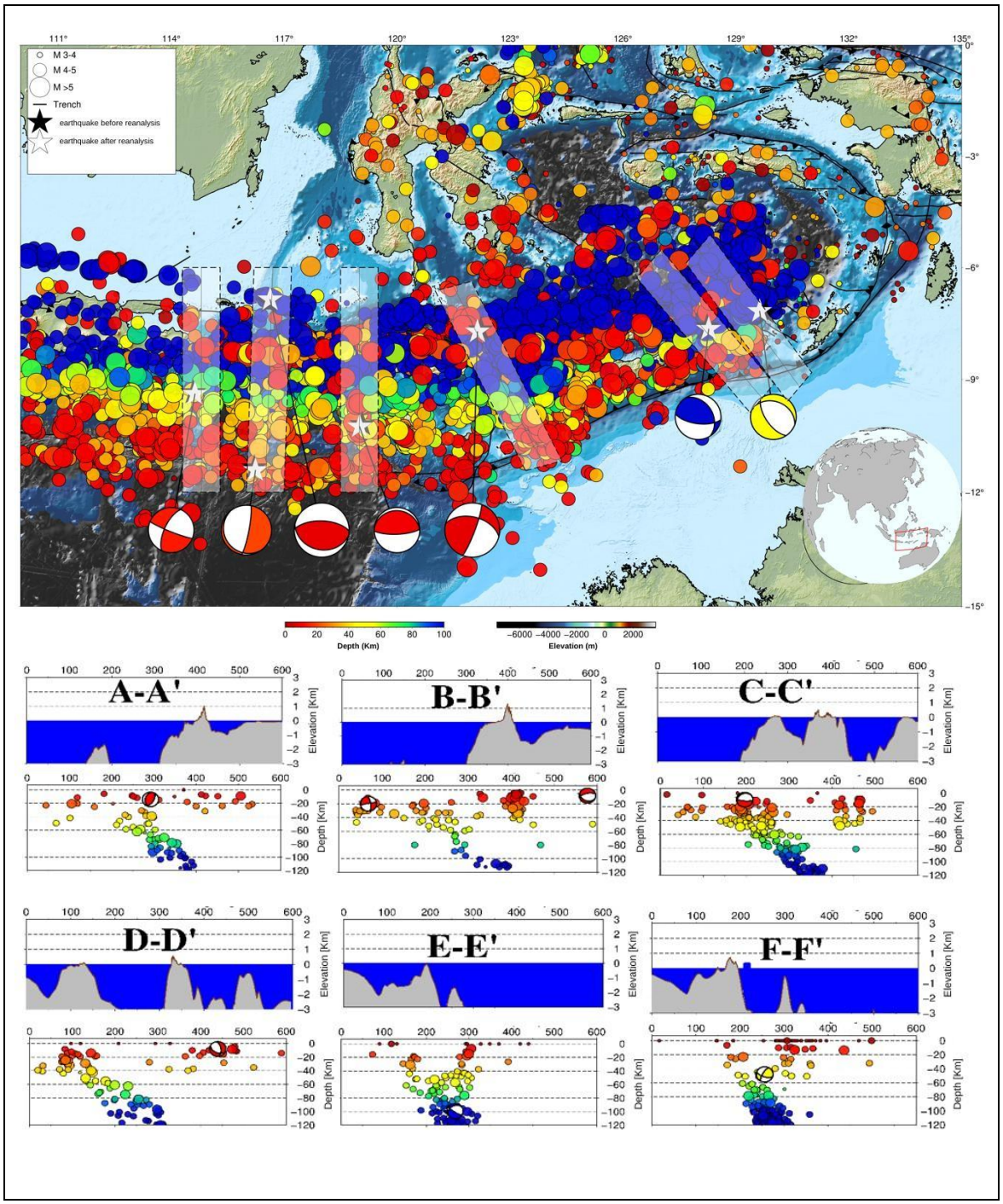

Fig 18. (a) Distribution of Relocated Earthquakes in the Indo-Australian Plate, (b) Cross-Sectional View

The Indo-Australian Plate region exhibits complex tectonic dynamics due to active interactions with surrounding plates, as shown in Figure 18a da 18b. Six cross-section profiles (A–A' to F–F') show earthquake depths <120 km and varying focal mechanisms: right-lateral strike-slip (A– A'), thrust faults (B–B', C–C', E–E', F–F'), and left-lateral strike-slip (D–D'), with hypocenters ranging from shallow to deep. Despite the compressive nature of subduction zones, normal faults also occur due to intraslab extension, outer-rise flexure, and slab rollback, generating local extensional environments. These observations indicate that both compressional and extensional regimes coexist, controlled by the internal dynamics and geometry of the subducting plate. Seismic hazard varies significantly across regions, with some areas exhibiting high seismic activity while others are relatively low. Large earthquakes can occur from both local and distant sources, and they can still impact areas located far from the epicenter (Khalqillah et al., 2025).

4. Conclusion

The waveform inversion results indicate that the refined earthquake parameters are reliable, as shown by the good fitting between synthetic and observed waveforms with misfit values of less than 0.5. Seismicity around the Indo-Australian Plate is dominated by earthquakes with magnitudes greater than 5, distributed along the subduction zone at varying depths and forming a Benioff zone pattern, reflecting active and complex subduction processes. The cross-sectional analysis further reveals diverse fault mechanisms, including right-lateral and left-lateral strike-slip, as well as thrust faults, highlighting the heterogeneous tectonic regime in the region.

Acknowledgements

The authors gratefully acknowledge the support of the staff and students of Syiah Kuala University and the Tsunami Disaster Mitigation Research Center (TDMRC) during data acquisition and analysis.

References

Alif, A. F., Nugroho, H., & Widiyantoro, S. (2021). Post-seismic deformation analysis following the 2016 Indian Ocean earthquake using GNSS data in western Indonesia. Geophysical Research: Solid Earth, 126(4), E2020JB020765.

Alif, S.M., Anggara, O., Perdana, R.S., Hasannah, U. & Azizah, F.N. (2024) 'Analysis of presumed land subsidence in the cities of Lampung Province using InSAR and GNSS data', Journal of Geoscience, Engineering, Environment, and Technology, 9(3), pp. 255–261. doi: 10.25299/jgeet.2024.9.3.14096.

Amad, R., Hansen, T.M., Jakobsen, M. & Chapman, M. (2020) On the full-waveform inversion of seismic moment tensors. Computers & Geosciences, 140, 104505.

Cesca, S., Heimann, S., Rivalta, E. and Dahm, T. (2017) 'Automated moment tensor inversion and earthquake characterization using probabilistic methods', Seismological Research Letters, 88(5), pp. 1482–1491.

DeMets, C., Gordon, R. G., & Argus, D. F. (2010). Geologically current plate motions. Geophysical Journal International, 181(1), 1–80.

Frohlich, C. (2001). Display and quantitative assessment of distributions of earthquake focal mechanisms. Geophysical Journal International, 144(2), 300–308.

Gibbons, A. D., Zahirovic, S., Müller, R. D., Whittaker, J. M., Yatheesh, V., & Lado-Insua, T. (2015). A tectonic model reconciling evidence for the collisions between India, Eurasia and intra-oceanic arcs of the central-eastern Tethys. Gondwana Research, 28(2), 451–492.

Gu, C., Toksöz, M. N. & Marzouk, Y. (2018) Waveform-based Bayesian full moment tensor inversion and uncertainty determination for the induced seismicity in an oil/gas field. Geophysical Journal International, 212(3), pp. 1963–1985.

Hall, R. (2002). Cenozoic geological and plate tectonic evolution of SE Asia and the SW Pacific. Journal of Asian Earth Sciences, 20(4): 353–431.

Harris, R. A. (2021). ifting and collision in the Banda Arc: The transition from subduction to arc-continent collision. Geological Society, London, Special Publications, 532(1), 1–35.

Heimann, S., Isken, M., Kühn, D., Sudhaus, H., Steinberg, A., Daout, S., Cesca, S., Vasyura-Bathke, H. & Dahm, T. (2018) Grond – A probabilistic earthquake source inversion framework. GFZ Data Services.

Heimann, S., Vasyura-Bathke, H., Sudhaus, H., Isken, M., Kriegerowski, M., Steinberg, A. & Dahm, T. (2019) 'A Python framework for efficient use of pre-computed Green's functions in seismological and other physical forward and inverse source problems', Solid Earth, 10(6), pp. 1921–1935. doi: 10.5194/se-10-1921-2019.

Hidayati, S. (2010). Pengantar Seismologi Gempabumi. Badan Pengkajian dan Penerapan Teknologi (BPPT).

H Simanjuntak and Muksin Umar, A. V. (2018). Analisis Mekanisme Fokal Menggunakan Inversi Waveform; Studi Kasus Gempa Bumi Pidie Jaya 7 Desember 2016. J. Aceh Phys. Soc, 7(3), 127–132.

Irwandi, Z., Zulfakriza, Muzli, Hassan, H.M. & Okubo, M. (2025) 'Seismic Hazard for Regional-Scale Sumatra Island Based on Realistic Physical Computation of Seismic Wave Propagation', Journal of Geoscience, Engineering, Environment, and Technology, 10(2).

Khalqillah, A., Umar, M., Simanjuntak, A.V.H., Jihad, A. & Banyunegoro, V.H. (2025) 'Seismic Hazard Estimation for Sumatra and Kalimantan Region Using Event-Based Probabilistic Seismic Hazard Analysis (EB-PSHA)', Journal of Geoscience, Engineering, Environment, and Technology, 10(3), pp. 329–337.

Lubis, A. M., Subarya, C., Meilano, I., & Nugraha, A. D. (2020). Re-evaluation of the Indo-Australian Plate motion using 23 years of GPS observations (1994–2016). Geoscience Letters, 7(1), 12.

McCaffrey, R. (2009). The tectonic framework of the sumatran subduction zone. Annual Review of Earth and Planetary Sciences, 37(November 2008), 345–366.

Müller, R. D., Zahirovic, S., Williams, S. E., Cannon, J., Seton, M., Bower, D. J., Tetley, M. G., Heine, C., Le Breton, E.,Liu, S., Russell, S. H. J., Yang, T., Leonard, J., & Gurnis, M. (2019). A Global Plate Model Including Lithospheric Deformation Along Major Rifts and Orogens Since the Triassic. Tectonics, 38(6), 1884–1907.

Petersen, G. M., Cesca, S., Heimann, S., Niemz, P., Dahm, T., Kühn, D., Kummerow, J., & Plenefisch, T. (2021). Regional centroid moment tensor inversion of small to moderate earthquakes in the Alps using the dense AlpArray seismic network: Challenges and seismotectonic insights. Solid Earth, 12(6), 1233–1257.

Petersen, M.D., Dewey, J., Hartzell, S., Mueller, C., Harmsen, S., Frankel, A.D. and Rukstales, K. (2004) 'Probabilistic seismic hazard analysis for Sumatra, Indonesia and across the Southern Malaysian Peninsula', Tectonophysics, 390(1-4), pp. 141–158.

Qadariyah, Q., Simanjuntak, A. V. H. & Umar, M. (2018). Analysis of Focal Mechanisms Using Waveform Inversion; Case Study of Pidie Jaya Earthquake December 7, 2016. Journal of Aceh Physics Society, **7**(3)

Reynolds, J. M. (2011). An Introduction to Applied and Environmental Geophysics. In European Space Agency, (Special Publication) ESA SP (2nd Editio, Issue 606). John Wiley & Sons, Ltd.

Shearer, P. M. (2009). Introduction to Seismology (2nd ed.). Cambridge : Cambridge University Press, New York.

Stein, S. and M. W. (2003). An Introduction to Seismology, Earthquakes, and Earth Structure. Blackwell Publishing Utd. United Kingdom.

Stern, R. . (2002). Subduction zones. Reviews of Geophysics, 40(4), 3–1–3-38.

Sunarjo, D. (2012). Gempabumi Edisi Populer. Jakarta, BMKG.

Tregoning, P., Lambeck, K., Stolz, A., Morgan, P., McClusky, S. C., Van Der Beek, P., McQueen, H., Jackson, R. J., Little, R. P., Laing, A., & Murphy, B. (1998). Estimation of current plate motions in Papua New Guinea from Global Positioning System observations. Journal of Geophysical Research: Solid Earth, 103(6), 12181–12203.

Van Hinsbergen, D. J. J., Steinberger, B., Doubrovine, P. V., & Gassmöller, R. (2018). cceleration and deceleration of India–Asia convergence since the Cretaceous: Roles of mantle plumes and continental collision. Nature Geoscience, 11, 516–521.

Wang, K., Hu, Y., & He, J. (2012). Deformation cycles of subduction earthquakes in a viscoelastic Earth. Nature, 484(7394), 327–332.